Supporting Information

Reprogrammable, reprocessible and self-healable liquid crystal elastomer with exchangeable disulfide bonds

Zhijian Wang,[†] Hongmiao Tian,[†,§] Qiguang He,[†] and Shengqiang Cai*[†,‡]

† Department of Mechanical and Aerospace Engineering, University of California, San Diego, La Jolla, CA 92093, USA
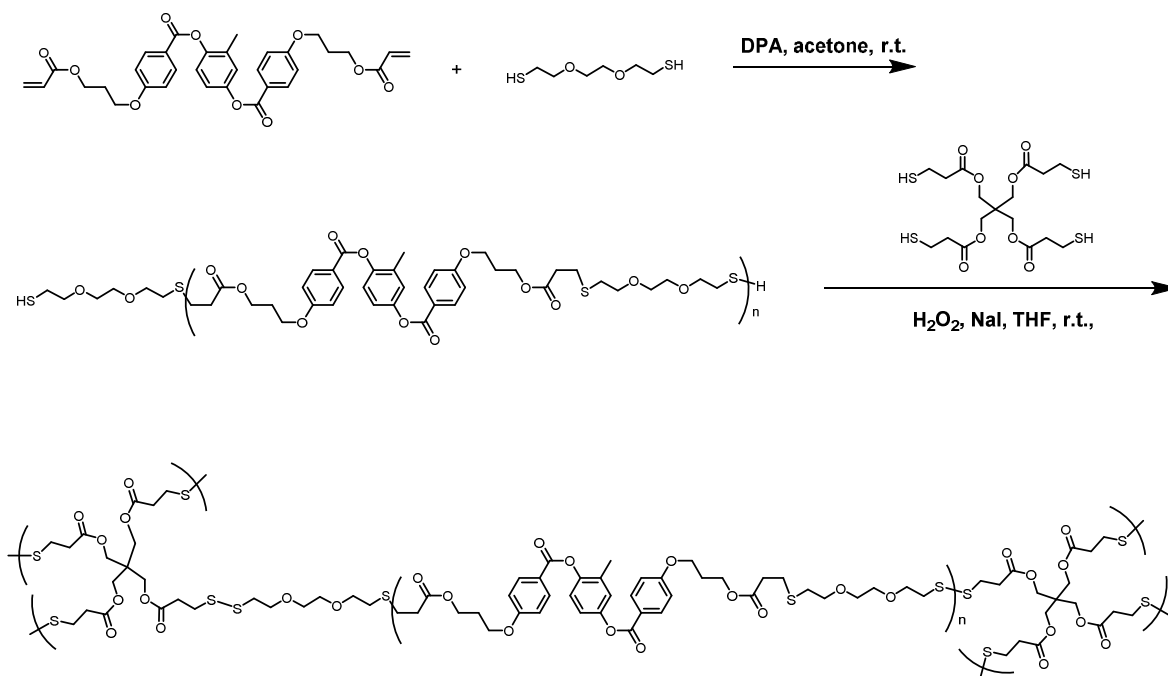
‡ Materials Science and Engineering Program, University of California, San Diego, La Jolla, CA 92093, USA

§ Micro- and Nano-technology Research Center, State Key Laboratory for Manufacturing Systems Engineering, Xi'an Jiaotong University, 28 Xianning Road, Xi'an, 710049, P. R. China

* Corresponding author

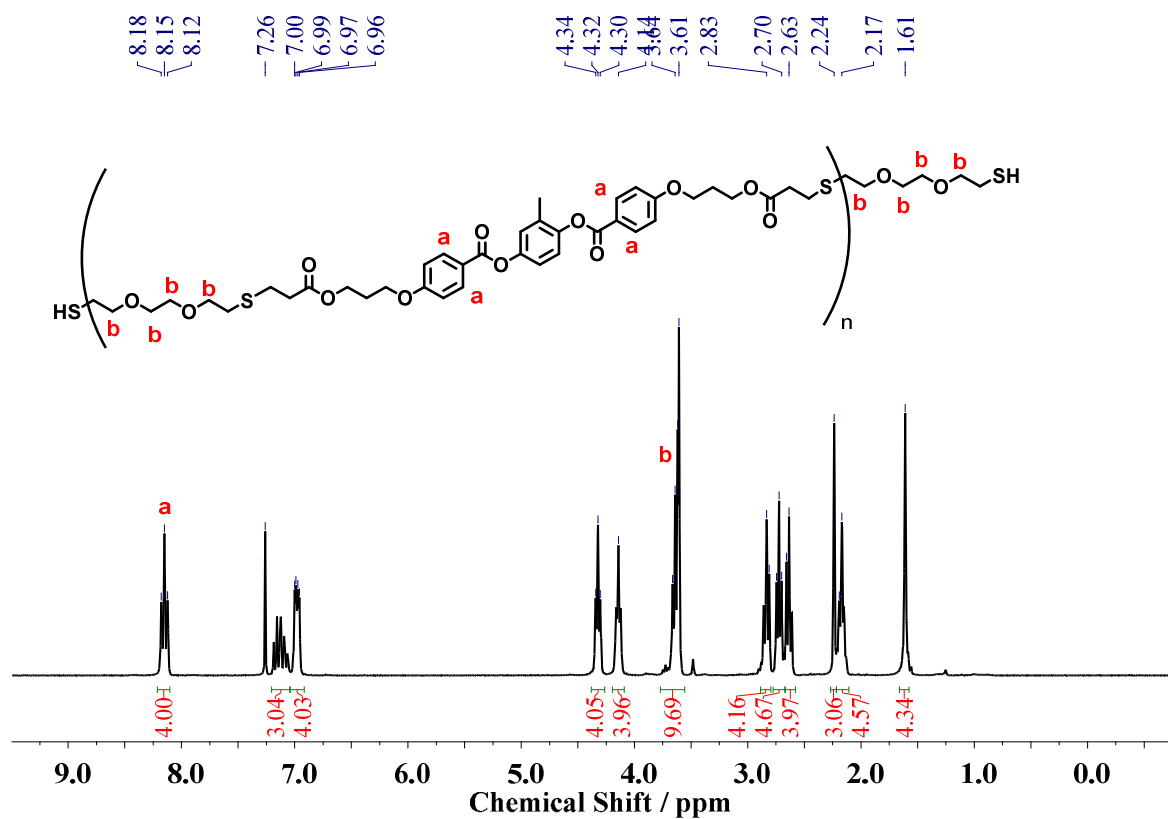E-mail: shqcai@ucsd.edu (Shengqiang Cai)

Scheme S1. Synthetic route for SS-LCE.

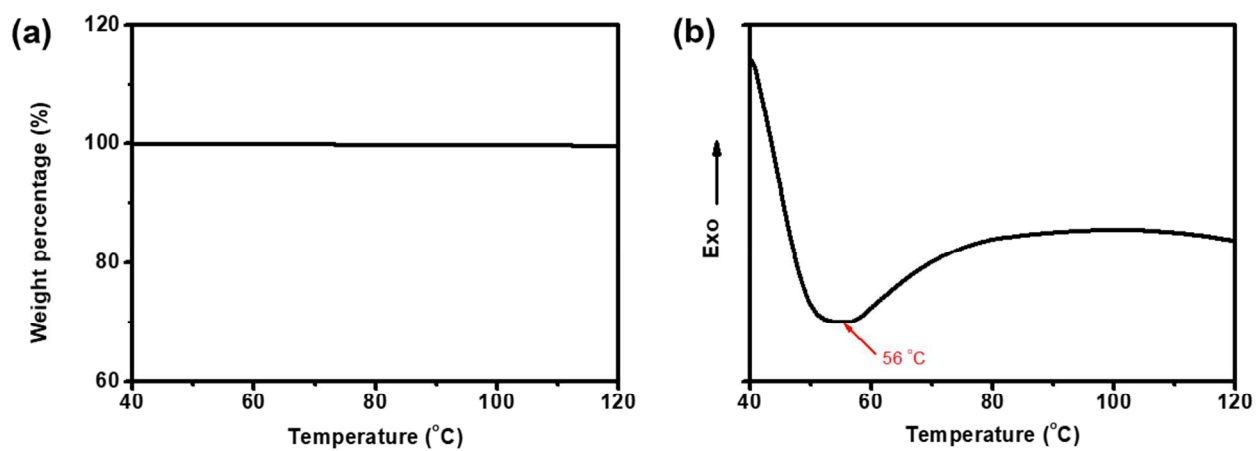Figure S1. ^{1}H NMR spectrum of the oligomer.

Figure S2. (a) TGA and (b) DSC curve of oligomer on the heating scan at a heating rate of 10.0 $^{\circ}$C /min under nitrogen atmosphere.
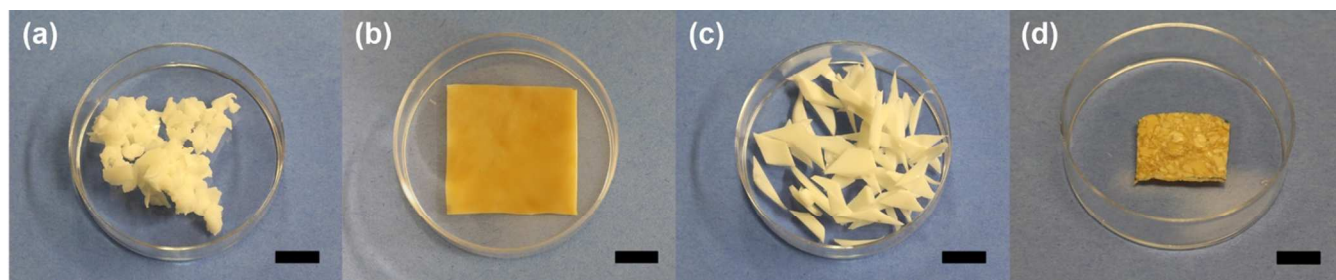

Figure S3. Photographs of SS-LCE-1 sample (a) before and (b) after hot-compression and LCE without disulfide bonds (c) before and (d) after hot-compression. Scale bar: 1 cm.
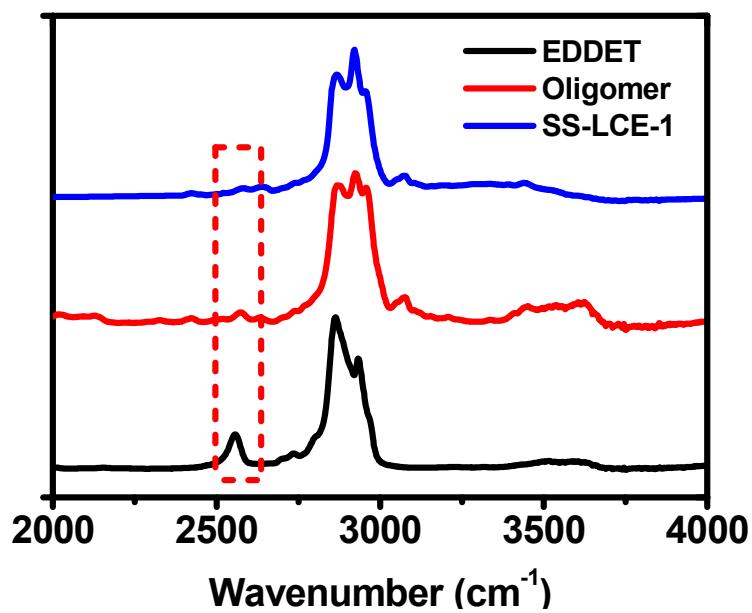
Figure S4. FT-IR spectra of EDDET (black line), oligomer (red line) and SS-LCE-1 (blue line).
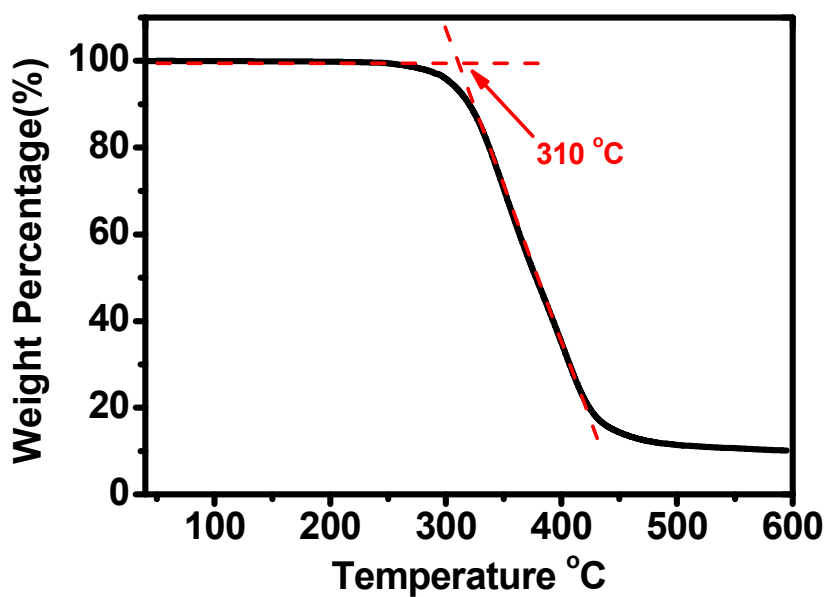

Figure S5. TGA curve of SS-LCE-1 at a heating rate of 10.0 $^{\circ}$C /min under nitrogen atmosphere.
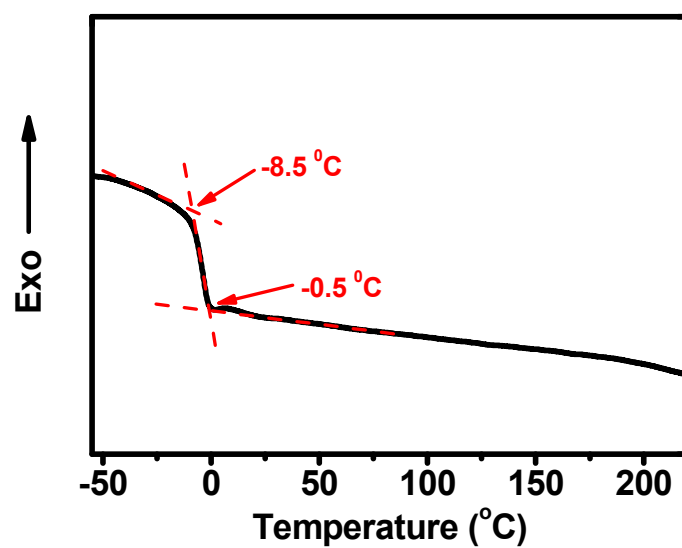
Figure S6. DSC curve of SS-LCE-1 on the heating scan at a heating rate of 10.0 °C /min under nitrogen atmosphere.
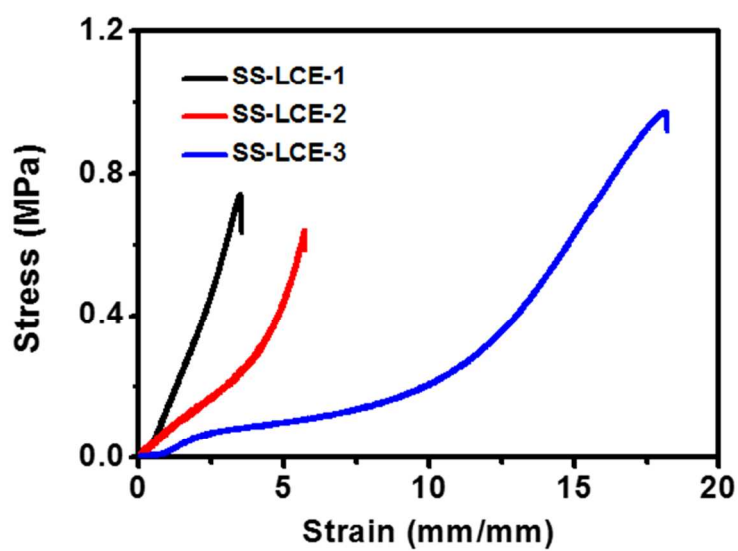

Figure S7. Stress-strain curves of SS-LCE samples with different crosslinking densities.
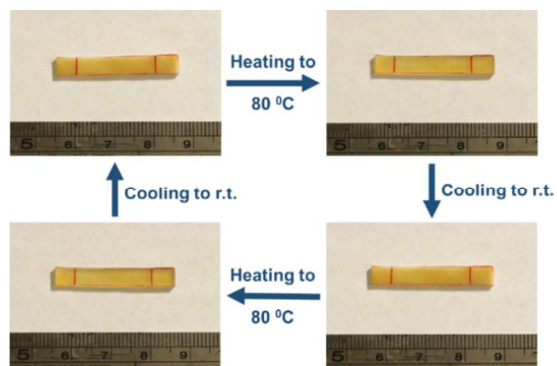
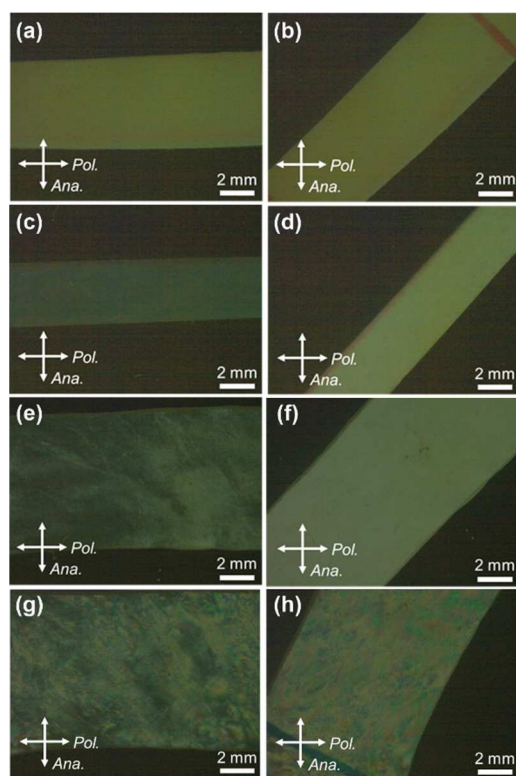Figure S8. Polydomain SS-LCE-1 during heating and cooling process.

Figure S9. Polarized optical microscope images of (a,b) polydomain SS-LCE-1, (c,d) stretched SS-LCE-1, (e,f) monodomain SS-LCE-1 and (g,h) monodomain SS-LCE-1 films at 80 °C with two different angles with respect to the analyzer.
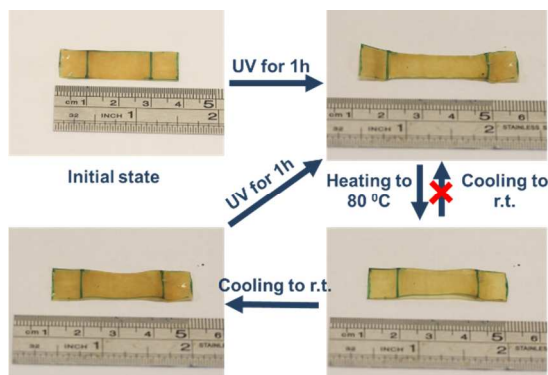
Figure S10. Actuation behavior of monodomain SS-LCE-2 obtained from UV irradiation during heating and cooling process.
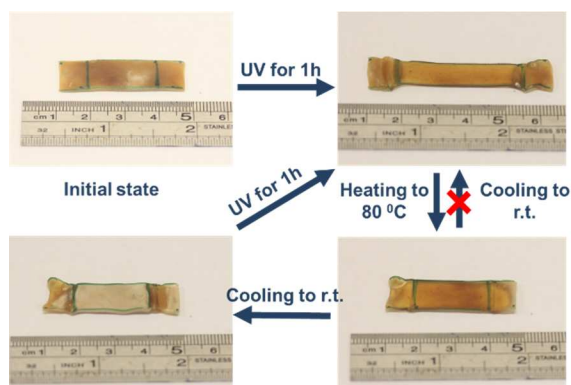

Figure S11. Actuation behavior of monodomain SS-LCE-3 obtained from UV irradiation during heating and cooling process.
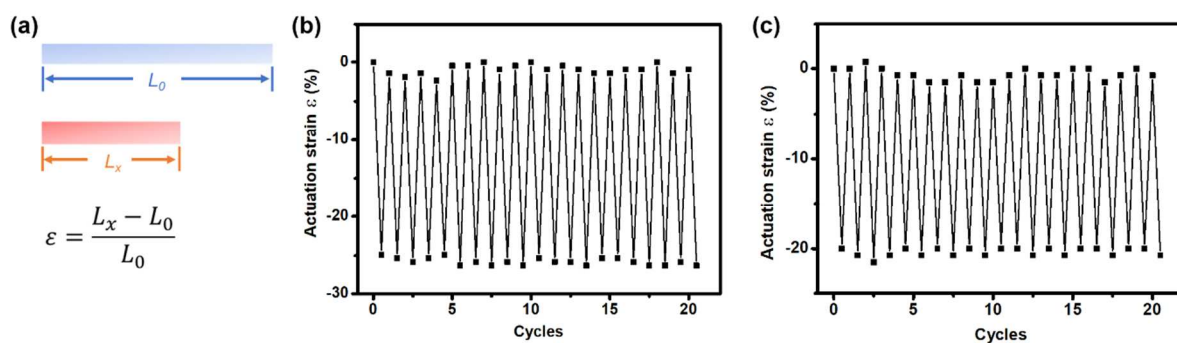

Figure S12. (a) Definition of actuation strain. Cyclic actuation tests of (b) UV programmed disulfide LCE and (c) thermally programmed disulfide LCE. The specimen was cyclically heated to 80 °C and then cooled down to the room temperature. The length of the specimen was recorded.
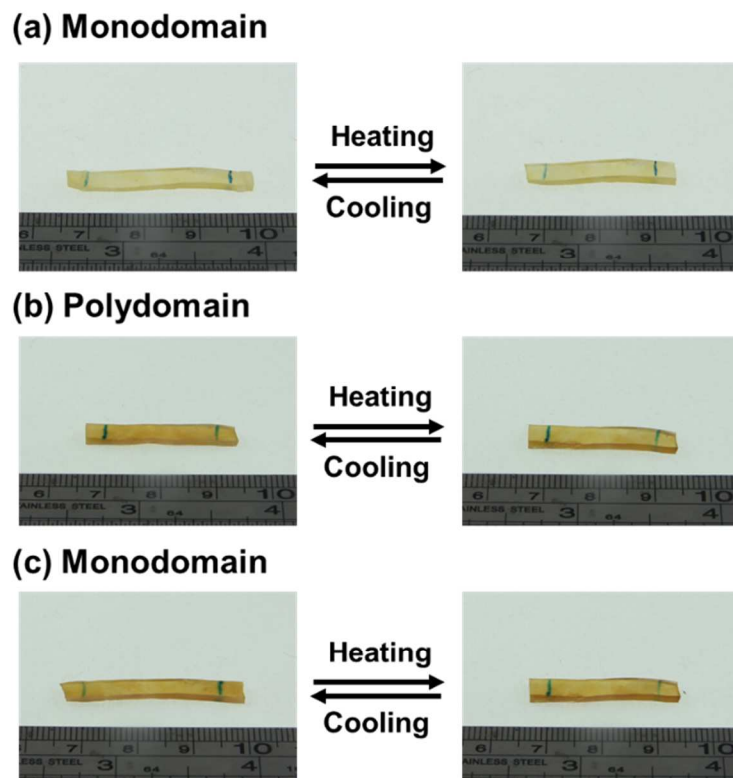
Figure S13. Reprogrammability of SS-LCE-1. Reversible actuation behavior of (a) UV-programmed monodomain LCE, (b) polydomain LCE obtained by thermally reprogrammed from monodomain LCE and (c) monodomain LCE obtained by thermally reprogrammed from polydomain LCE. All the images are the same LCE sample. The as-prepared SS-LCE-1 was stretched and irradiated under UV light for 1h. (a) The irradiated specimen showed reversible actuation behavior under cyclic heating and cooling, which means that the specimen transited from polydomain to active monodomain under UV irradiation. Then the free standing monodomain specimen was heated to 180 °C for 20 min and cooled to the room temperature. The reversible actuation behavior can be erased under high temperature. It recovered to the polydomain state and could not show reversible contraction and expansion behavior (b). When the polydomain sample was heated to 180 °C for 20 min, then stretched and cooled to the room temperature, it can be fixed into active monodomain state again. The thermally treated specimen would show reversible actuation behavior (c).
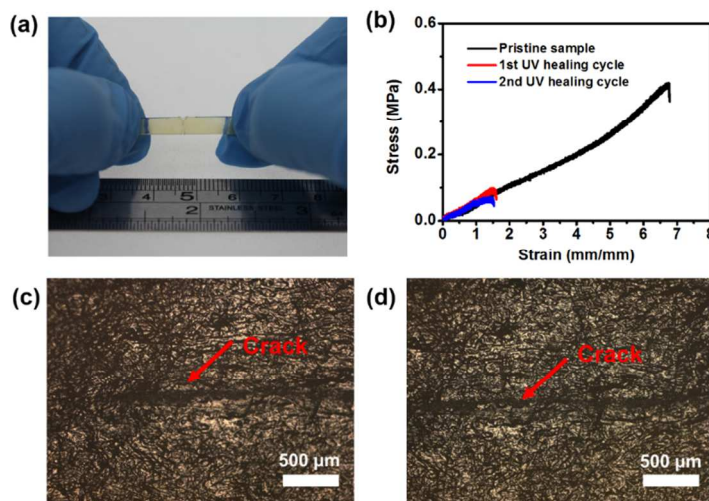
Figure S14. (a) Photograph of UV healed SS-LCE specimen. The healed specimen failed after stretching to 2 times of initial length; (b) Stress-strain curves of healed SS-LCE-1 upon UV illumination. The specimen was placed under UV lamp for 3 hours for each cycle; Microscopic images of crack in SS-LCE-1 (c) before and (d) after UV illumination for 3 hours.
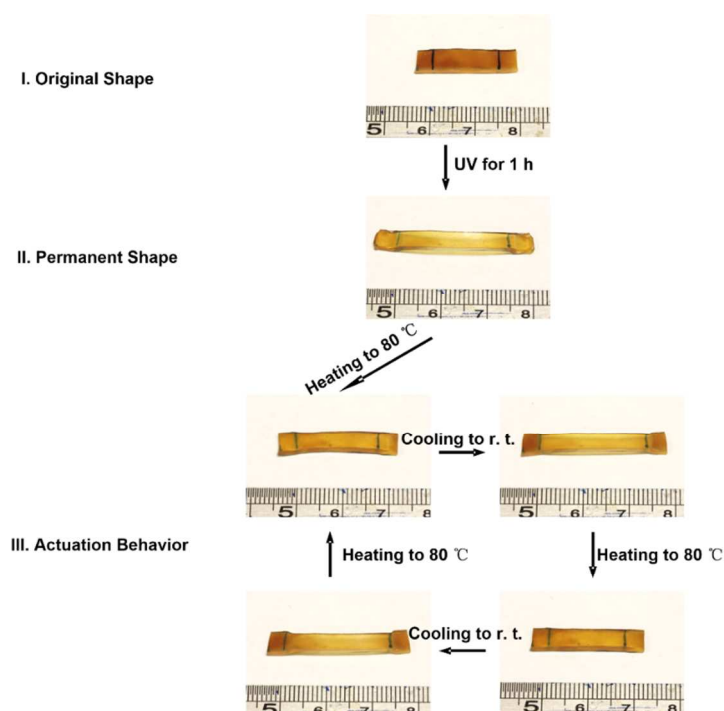

Figure S15. Demonstration of long-term durability of SS-LCE specimen. The specimen can keep its UV-reprogrammable property after stored in the ambient temperature for 3 months.